




Article

Research on Permeability Coefficient of Fine Sediments in Debris-Flow Gullies, Southwestern China

Qinjun Wang^{1,2,3,*} , Jingjing Xie^{1,2}, Jingyi Yang^{1,2}, Peng Liu^{1,2}, Dingkun Chang^{1,2} and Wentao Xu^{1,2,4}

- ¹ Key Laboratory of Digital Earth Science, Aerospace Information Research Institute, Chinese Academy of Sciences (CAS), Beijing 100094, China; xiejingjing19@mailsucas.ac.cn (J.X.); yangjingyi211@mailsucas.ac.cn (J.Y.); liup@aircas.ac.cn (P.L.); changdingkun20@mailsucas.ac.cn (D.C.); 07182642@cumt.edu.cn (W.X.)
- ² Yanqi Lake Campus, University of Chinese Academy of Sciences, Beijing 101408, China
- ³ Key Laboratory of the Earth Observation of Hainan Province, Aerospace Information Research Institute, CAS, Hainan Research Institute, Sanya 572029, China
- ⁴ School of Environment and Spatial Informatics, China University of Mining and Technology, Xuzhou 221116, China
- * Correspondence: wangqj@radi.ac.cn

Abstract: Fine sediments in debris-flow gullies are quaternary sediments with a particle size of less than 2 mm. Since they are easy to suspend in flowing water, their stability plays a key “probe” role in early debris-flow warning. The permeability coefficient is the main internal control factor of fine sediment stability in debris flow. However, there is no quantitative model between the permeability coefficient and its influencing factors, which seriously affects the quantitative evaluation of debris flow sediments. Taking the debris-flow gullies in Laobeichuan County, Sichuan Province, China as the research area, we carried out experiments on the permeability coefficient and its influencing factors. A model between the permeability coefficient and its influencing factors was established by the least-squares multivariate statistical analysis method. The results showed that cohesion was the closest factor to the permeability coefficient, followed by porosity and density. Each factor passed the t-test and significantly correlated with the model in 99.99% probability. With a correlation coefficient of 0.72, the model had a good prediction ability. Therefore, the model not only provides a theoretical basis for analyzing the stability of fine sediments in Laobeichuan County, but also points out the direction for detecting the fine sediment stability in debris-flow gullies.

Keywords: geological hazards; permeability coefficient; cohesion; porosity; density



Citation: Wang, Q.; Xie, J.; Yang, J.; Liu, P.; Chang, D.; Xu, W. Research on Permeability Coefficient of Fine Sediments in Debris-Flow Gullies, Southwestern China. *Soil Syst.* **2022**, *6*, 29. <https://doi.org/10.3390/soilsystems6010029>

Academic Editor: Abdul M. Mouazen

Received: 28 January 2022

Accepted: 14 March 2022

Published: 18 March 2022

Publisher's Note: MDPI stays neutral with regard to jurisdictional claims in published maps and institutional affiliations.



Copyright: © 2022 by the authors. Licensee MDPI, Basel, Switzerland. This article is an open access article distributed under the terms and conditions of the Creative Commons Attribution (CC BY) license (<https://creativecommons.org/licenses/by/4.0/>).

1. Introduction

In recent years, affected by tectonic activities and climate changes, the activity of debris flow has increased and led to rising casualties and economic losses. Therefore, it has become one of the most dangerous mountain hazards. Debris flow is a special flood containing a large amount of soils and stones caused by heavy rain, snow (ice) melting, or other natural hazards. With the characteristics of a wide area, a large amount of materials, and strong destructive power, it often leads to the collapse of houses and the destruction of highway facilities, and thus causes serious threat to the life and property of local people [1]. For example, the “8.20” Sichuan debris flow, one of the top 10 geological disasters of China in 2019, affected 446,000 people, with 26 dead and 19 missing. Some infrastructure, such as roads, water conservancies, and power facilities, was seriously damaged, resulting in a direct economic loss of CNY 15.89 billion (USD 2.51 billion) [2]; the serious Zhouqu debris flow on 7 August 2010 caused 1435 people dead and 330 people missing, with a direct economic loss of CNY 400 million (USD 63.28 million) [3]; the Beichuan debris flow on 24 September 2008 buried most of the buildings in Laobeichuan County, resulting in 42 people dead or missing and more than 4000 people trapped [4].

Therefore, rapid and accurate early warning of debris flow plays an important role not only in ensuring the safety of people's lives and property, but also in social and economic development of mountainous areas.

In this article, fine sediments refer to the Quaternary sediments with particle sizes of less than 2 mm, which mainly include floodplain sediments in rivers and fine residual slope sediments at the foot of mountains. With loose structure and large porosity, their stability is closely related to the initial water volume inducing debris flow and plays a key "probe" role in debris-flow early warning [5–14].

Therefore, debris-flow early warning needs to quickly and accurately detect the stability of these fine sediments. References show that their stability is mainly affected by internal and external factors. Internal factors mainly include the permeability coefficient, cohesion, and internal friction angle; external factors mainly include water resources (rainfall, runoff, etc.), landform conditions (slope, confluence areas, etc.), surface coverage, etc. [15–17].

The permeability coefficient is also called hydraulic conductivity. In the study area, fine sediments on the beach edge along the riverside are sieved by water and loosely deposited; their components and particle sizes change little, so we consider them to be isotropic. As shown in formula (1), the permeability coefficient is defined as the unit flow under the unit hydraulic gradient, which indicates the difficulty of fluid passing through the pore skeleton. The higher the permeability coefficient is, the stronger the soil permeability becomes. As an internal control factor of sediment stability, it mainly reflects the size, number, and connectivity of soil pores [18].

$$K_T = 2.3 \frac{aL}{At} l g \frac{h_1}{h_2} \quad (1)$$

where K_T is the permeability coefficient at temperature T , a is the cross-sectional area of the variable head pipe (cm^2), L is the height of the sample (cm), A is the cross-sectional area of the sample (cm^2), t is the time (s), h_1 is the starting water head (cm), and h_2 is the ending water head (cm).

In addition to the application in debris-flow early warning, many disasters, such as piping have occurred in dam engineering because of the failure to fully consider the effect of sand permeability. Therefore, analysis of soil permeability is not only helpful to discover the hazard mechanism, but it can also provide a scientific basis for geological hazards prevention and engineering facilities construction [19–24].

As to the study area, the spatial-temporal evolution characteristics of landslides [25], the sensitivity analysis of debris flow on environmental factors [26], and the relationship between debris flow and environmental factors [27] have been studied. However, there is no quantitative model between the permeability coefficient and its influencing factors of the fine sediments in debris-flow gullies. Therefore, enhancing the research on the permeability coefficient of fine sediments in a debris-flow gully, discovering its influencing factors, and establishing a quantitative model between the permeability coefficient and its influencing factors are not only the basic requirements for revealing the soil stability mechanism, but also of great significance for establishing the soil stability detection model of gully sediments.

2. Materials and Methods

2.1. Study Area

With altitudes of 600–1800 m, the study area is mainly located near Laobeichuan County, adjacent to Jiangyou City in the east, Anxian in the south, Maoxian in the west, and Songpan County and Pingwu County in the north. With the geographic coordinates of $104^\circ 23' - 104^\circ 31.7' \text{ E}$, $31^\circ 48.5' - 31^\circ 53.5' \text{ N}$, it covers an area of about 140 km^2 (Figure 1).

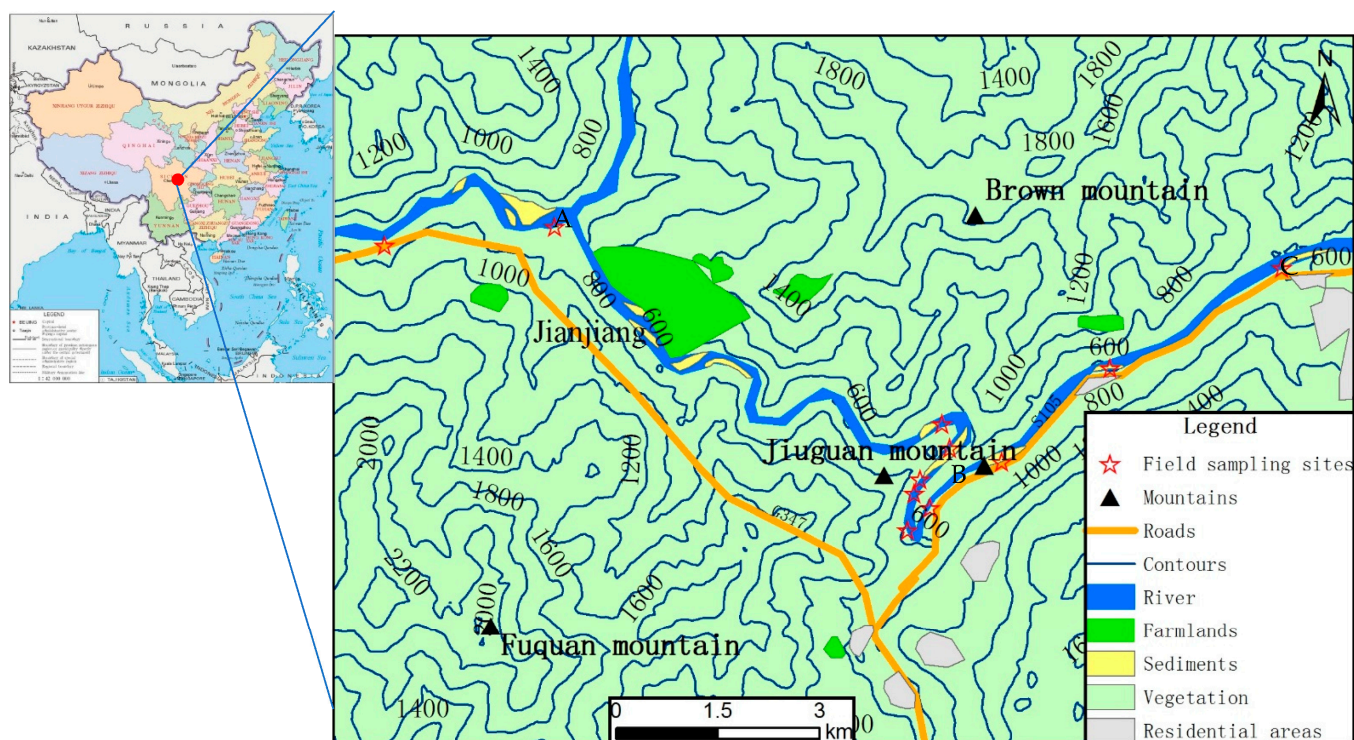


Figure 1. Location map of study area (map on the left shows the location of study area in China).

According to the Köppen climate classification standard, the climate of the study area is the humid subtropical climate (Cfa) with four seasons, mild climate, and annual average temperature of 15.6 °C. Its annual average rainfall is 1399.1 mm, with a daily maximum rainfall intensity of 301 mm and an hourly maximum rainfall intensity of 62 mm. The rainfall is concentrated from June to September, accounting for 74% of the annual rainfall [4].

Because the Wenchuan earthquake happened here in 2008, its soil cover is erodible [4], and thus leads to frequent debris flow. On 20 August 2019, 11 July 2018, 28 July 2016, 6 July 2013, 17 August 2011, and 24 September 2008, six serious debris-flow hazards have taken place since the Wenchuan earthquake happened. As a result, nearly 10,000 people had to leave their homes, more than half of the buildings in Laobeichuan County were buried, and a large number of farms in the disaster area were flooded or destroyed.

2.2. Methods

As shown in Figure 2, the flowchart of this research includes “Study area and background data acquisition-Parameter measurement experiments-Model establishment-Results”.

(1) Study area and background data acquisition

We obtained the geological and meteorological data and the land-use map, as well as Gaofen (GF-2) [28] and other high-resolution remote sensing data. Based on this, the improved depth learning method was used to extract the map of fine sediments in the study area [1]. A database of internal control factors for the stability of sediments was established.

(2) Parameter measurement experiments

According to the standard for investigation of landslides, landslips, and debris flows (DZ/T 02161-2014) [29], and the technical guide for soil sampling (GB/T 36197-2018) [30], samples were collected in the field.

According to the standard for geotechnical experiments (SL237-1999) [31], parameter measurement experiments were carried out that included the permeability coefficient and its influencing factors in measurement experiments, such as for density, moisture, minerals, elements, particle size, porosity, and shear strength.

(3) Model establishment

Based on the experimental data of permeability coefficient and its influencing factors, the function between permeability coefficient and each influencing factor was established first. Then, using the function, the mathematical transformation was carried out to ensure that the transformed permeability coefficient and each factor was of a linear relationship. Finally, the model between permeability coefficient and its multi-influencing factors was established by the least-squares multivariate statistical analysis method.

(4) Results

After establishing the model between permeability coefficient and its multi-influencing factors, whether to improve it or not was determined according to its accuracy. When the accuracy meets the requirements, the model is output. When it does not, it is necessary to analyze the causes and re-establish the model.

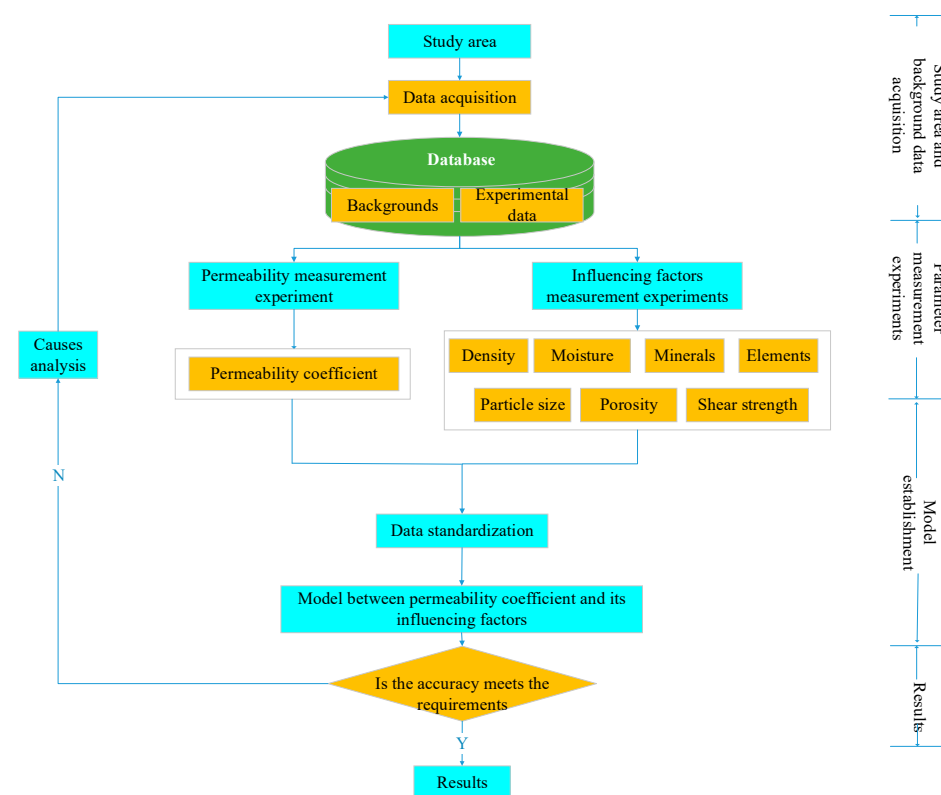


Figure 2. Technical flowchart.

2.3. Data Acquisition and Processing

2.3.1. Background Data

According to the rules of the basic geographic information database (GB/T 30319-2013) [32], meteorological and hydrological maps, geological maps, DEM/topographic maps, traffic maps, etc., were collected to establish a database of fine sediment stability.

In addition, GF-2 satellite remote sensing data was also obtained to design the sampling sites.

2.3.2. Samples

From 19–25 March 2021, we carried out a field investigation in Laobeichuna County along the Jianjiang for sampling. The sampling sites were designed according to the standard for investigation of landslides, landslips, and debris flows (DZ/T 0216-2014), and the technical guide for soil sampling (GB/T 36197-2018).

As shown in Figure 1, to reflect the distribution of the soil permeability coefficients in different locations we designed 11 sampling sites along the Jianjiang. A photo of sampling

site A in Figure 1 is shown in Figure 3. In each sampling site, we collected 15–20 samples according to its area. Finally, 200 samples were collected using a ring knife. Each sample has a volume of 600 mL and a weight of about 1 kg. With a diameter of 7 cm, and a depth of 5.2 cm, the volume of the ring knife is 200 mL. Using this, the sampling procedure for a soil sample was as follows: first, we cleaned the ring knife using a soft cloth. Then we put it into the sediments vertically. When it was full of soil, we pulled it out and cut off the over-flowing soil with another knife. Thus, a soil sample with a volume of 200 mL was collected. Finally, we immediately put the soil sample into a plastic bag and sealed it. After collecting three soil samples in the same plastic bag according to the above steps, we sealed the plastic bag and considered it as one sample with a volume of 600 mL and put it into a cotton bag. Finally, we recorded the sample number and its geographical location using a global positioning system (GPS) and wrote the sample number on the cloth sample bag with a marker.



Figure 3. Photo of sampling site A in Figure 1.

2.3.3. Parameter Measurement Experiments

The experiments on permeability coefficient and its influencing factors were carried out to get the permeability coefficient, density, moisture, minerals, elements, particle size, porosity, and shear strength. Based on the above data, the model between the permeability coefficient and its influencing factors was established to indicate the internal control mechanism of the fine sediment stability in the study area.

(1) Permeability coefficient measurement experiment

In this research, a TST-55 permeameter was used to measure the permeability coefficient of fine sediment according to geotechnical test rules (SL237-1999) (Figure 4).

The permeability coefficient was measured according to the instruction of the TST-55 permeameter. After the soil sample was prepared with its ring knife, we made water flow into the sample, then recorded the initial water head h_1 (cm), start timing t (s), the end water head h_2 (cm), and the terminal water temperature T ($^{\circ}\text{C}$). Finally, the permeability coefficient was calculated using formula (1) and the average value of four measurements was used as the final permeability coefficient. According to the above steps, the permeability coefficients of fine sediments are measured and shown in Figure 5.

It can be seen from the figure that the minimum permeability coefficient of fine sediments is 0.47 m/d and the maximum is 2.85 m/d, most of which is concentrated between 1.15–2.17 m/d, belonging to the category of medium permeability, which is stable under the conditions of non-heavy rain. There is some dependence between the sampling

locations and permeability coefficient. The average permeability coefficient is 1.4–1.6 m/d on both sides of Figure 1, such as sites A and C, which is less than that in the middle, such as site B, with a value of 2.1–2.3 m/d.

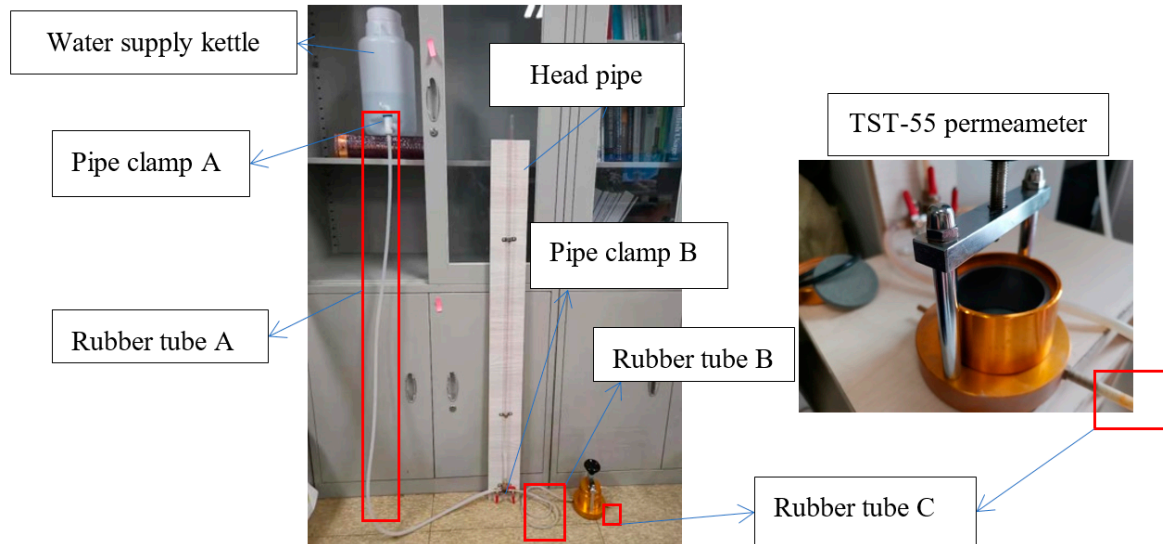


Figure 4. Permeability coefficient measurement experiment.

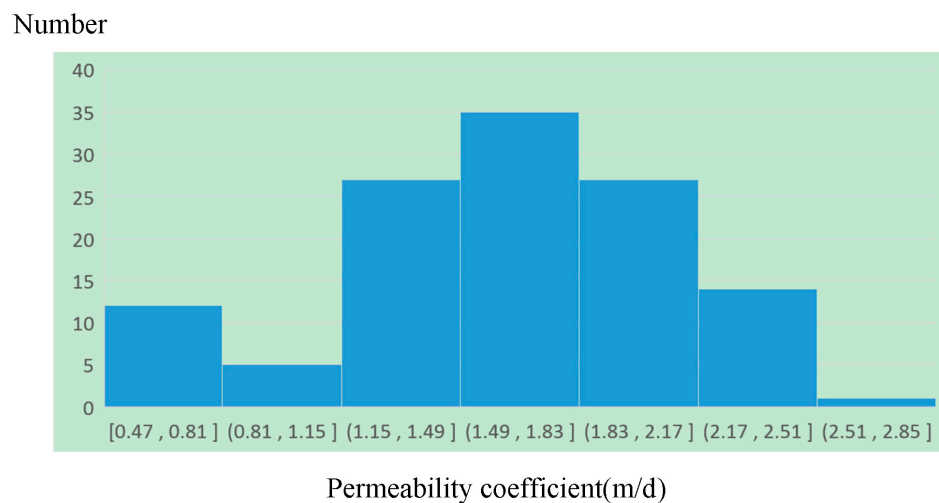


Figure 5. Histogram of fine sediment permeability coefficient.

(2) Measurement experiments on influencing factors of permeability coefficient

Investigations showed that the main influencing factors of the permeability coefficient included density, moisture, minerals, elements, particle size, porosity, and shear strength. Therefore, their measurement experiments were carried out as follows.

(a) Particle size measurement experiment

Particle size was measured by Microtrac S3500 laser particle size analyzer produced by Microtrac Inc., U.S. The range of the particle size of the analyzer is 0.02–2000 μm and that of the detection angle is 0.02–160°. The analyzer can eliminate the interference of refraction and reflected light between different particles to make the measurement results more accurate.

Since our research objects are fine-grained sediments with particle sizes of less than 2 mm, during the process of measuring we first dry the sample and remove the non-fine sediment, such as little stones, short branches, or grass, using a sieve with a mesh size of 2 mm (10 meshes). Then we disperse the sample in a delivery controller and flow it

through the Microtrac S3500 system according to its user's manual. Finally, the analyzer determines the particle size automatically. In the output results, it will list the measurement channel particle sizes ranging from 0.289 to 2000 μm and their corresponding content in each measurement channel for a sample.

To calculate the correlation coefficient between different factors, such as the permeability coefficient, density, particle size, porosity, etc., the particle size of a sample is represented by the average value from different measurement channel particle sizes and their corresponding content. So, the particle size of a sample is determined by the sum of measured channel particle size multiplying the content using the following equation:

$$d = \sum_{i=1}^n d_i * p_i$$

where d is the particle size of a sample, i is the i th measurement channel, n is the number of measurement channels, d_i is the particle size of i th measurement channel, like 13.08 μm , 176 μm , etc., and p_i is the content of the corresponding particle size in the i th measurement channel, like 3.5%, 4.51%, etc.

Histogram of fine sediments particle size is shown in Figure 6.

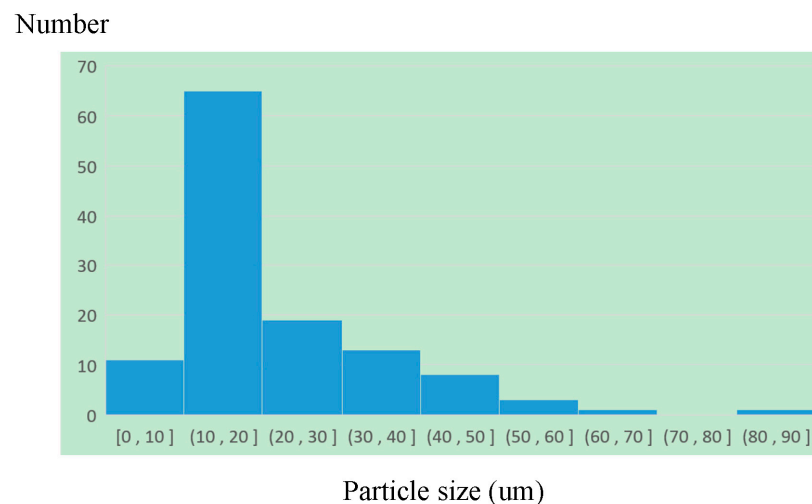


Figure 6. Histogram of fine sediment particle size.

It can be seen from the figure that the minimum particle size of soil samples in the study area is 0.45 μm and the maximum is about 90 μm , most of which is mainly distributed 10–20 μm . According to the standard for the engineering classification of soil (GB/T 50145-2007) [33], they belong to silt loams. As shown in Table 1, the statistical results showed that it had no significant correlation with other factors, such as moisture, porosity, shear strength, the permeability coefficient, etc.

Table 1. Table of correlation coefficients.

	Particle Size	Montmorillonite	K	Fe	Moisture	Density	Porosity	Permeability Coefficient (p)	ln(p)	Internal Friction Angle	Cohesion
Particle size	1.00	−0.12	−0.05	−0.03	0.07	0.13	−0.04	0.00	0.00	−0.05	0.08
Montmorillonite	−0.12	1.00	−0.25	−0.32	0.37	0.31	0.18	0.00	−0.02	−0.04	−0.03
K	−0.05	−0.25	1.00	0.82	−0.74	−0.58	−0.42	0.16	0.20	−0.09	−0.04
Fe	−0.03	−0.32	0.82	1.00	−0.65	−0.56	−0.33	0.11	0.16	−0.15	−0.06
Moisture	0.07	0.37	−0.74	−0.65	1.00	0.80	0.70	−0.43	−0.48	−0.13	0.32
Density	0.13	0.31	−0.58	−0.56	0.80	1.00	0.38	−0.46	−0.51	−0.08	0.36
Porosity	−0.04	0.18	−0.42	−0.33	0.70	0.38	1.00	−0.46	−0.51	−0.10	0.29
Permeability coefficient (p)	0.00	0.00	0.16	0.11	−0.43	−0.46	−0.46	1.00	0.97	0.32	−0.56
ln(p)	0.00	−0.02	0.20	0.16	−0.48	−0.51	−0.51	0.97	1.00	0.31	−0.58
Internal friction angle	−0.05	−0.04	−0.09	−0.15	−0.13	−0.08	−0.10	0.32	0.31	1.00	−0.66
Cohesion	0.08	−0.03	−0.04	−0.06	0.32	0.36	0.29	−0.56	−0.58	−0.66	1.00

(b) Density measurement experiment

Density is a measurement of the compaction degree of soil particles under certain mass, which is closely related to soil permeability. In this experiment, an MDJ-300A solid densitometer is used for density measurement.

The histogram of soil density in the study area is shown in Figure 7.

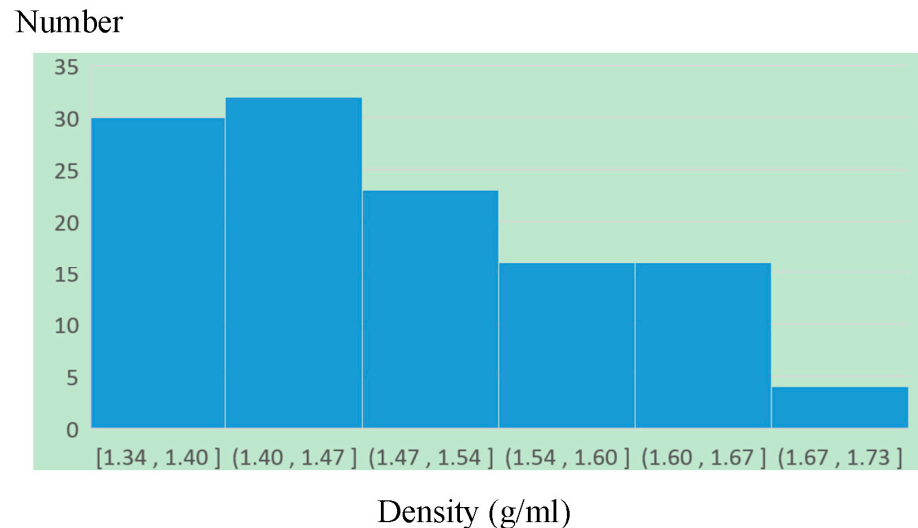


Figure 7. Histogram of fine sediment density.

It can be seen from the figure that the minimum density is 1.34 g/mL and the maximum is 1.73 g/mL, most of which is mainly distributed between 1.34–1.54 g/mL, belonging to the range of silt loams.

As shown in Table 1, with a correlation coefficient of 0.80, the density had a positive correlation with the moisture. However, with a correlation coefficient of -0.51 , the density had a negative correlation with the logarithm of the permeability coefficient.

(c) Minerals measurement experiment

Minerals were measured using a D8 Discover high-resolution X-ray diffractometer. According to the rules for geotechnical experiments (SL 237-1999), the minerals were measured and exported into the database through the steps of crushing, screening, sample preparation, loading, scanning, data acquisition, and processing in the laboratory.

The correlation analysis of various parameters is shown in Table 1: the main minerals in the study area are quartz (51%), feldspar (13%), and mica (7%). The secondary minerals are mainly montmorillonite (23%). With the correlation coefficient of 0.37, montmorillonite is correlated with the moisture.

(d) Element measurement experiment

‘Element’ is a general term for the same kind of atoms with the same number of protons. To discover the correlation between each element and the permeability coefficient in the study area, we carried out an element measurement experiment in which an INNOV C820 element analyzer was used to measure the content of elements. The results show that the main elements in the study area are iron and potassium, whose histograms are shown in Figure 8.

It can be seen from the figure that the minimum iron content is 2.16% and the maximum is 3.76%, most of which is between 2.56–3.16%. The minimum potassium content is 0.032% and the maximum is 0.074%, most of which is between 0.038–0.056%.

The results were exported into the database, and the correlation analysis of various parameters was carried out. As shown in Table 1, with a correlation coefficient of 0.82, iron (Fe) is positively related to potassium (K). However, with correlation coefficients of -0.65 and -0.56 , this has negative correlations with the moisture and density, respectively.

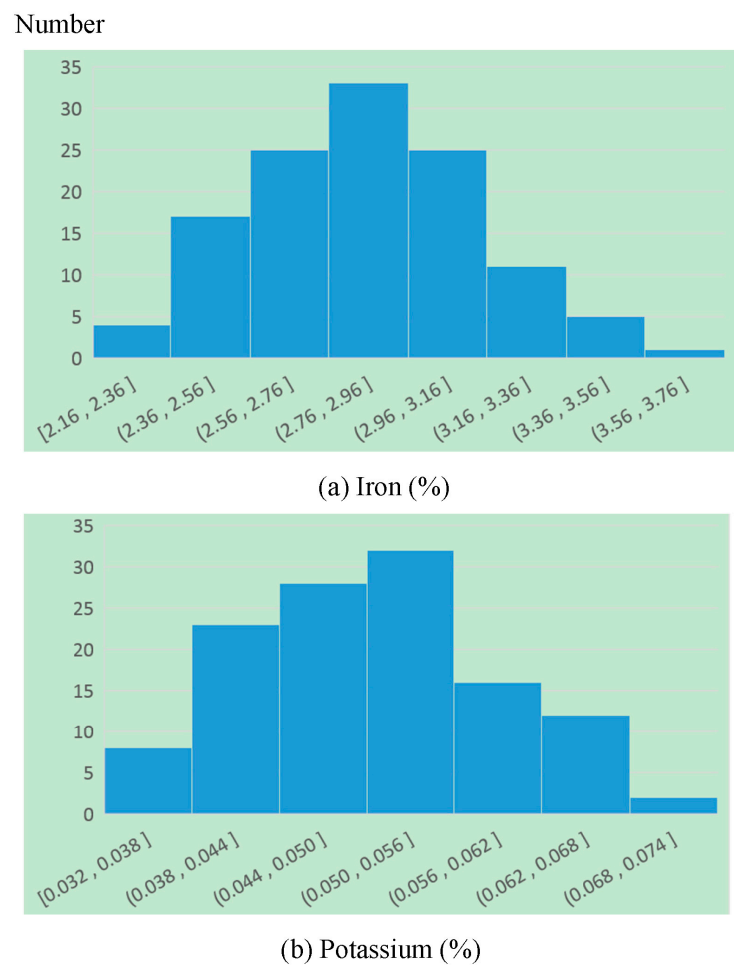


Figure 8. Iron (a) and potassium (b) histograms of fine sediments.

(e) Moisture measurement experiment

Moisture refers to how much water is in 100 g of dried soil. When the porosity in a sample is constant, the soil moisture has a great influence on the residual porosity, and then affects the soil permeability. In this experiment, an electro-thermal constant temperature drying oven is used to measure the soil moisture through the following steps: ① put m_0 g soils into the aluminum box and put this into the drying oven; ② turn on the switch, and set temperature to 110 °C and when the temperature rises to the set temperature, the drying oven enters the constant temperature mode, and the drying time is not less than 8 h; ③ after fully drying, take out the aluminum box and record the dried sample weight in m_1 g; and ④ calculate moisture with the following formula: $w = (m_0/m_1 - 1) \times 100\%$.

According to the above steps, the soil moisture in the study area was measured as shown in Figure 9.

It can be seen from the figure that the minimum and maximum moisture in the study area are 4.01% and 30.69%, respectively, most of which is concentrated in 4.01–9.35%, belonging to medium drought level in agriculture and grey entropy in the soil moisture category.

The results were exported into the database, and the correlation analysis of various parameters was carried out. As shown in Table 1, with correlation coefficients of 0.80 and 0.70, the moisture is positively correlated with the density and the porosity, respectively. However, with a correlation coefficient of -0.74 , it has a negative correlation with the potassium (K).

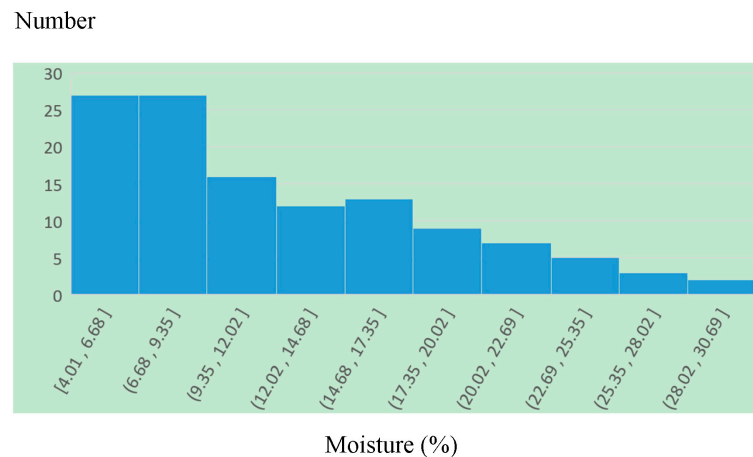


Figure 9. Histogram of fine sediment moisture.

(f) Porosity measurement experiment

Soil porosity is the volume percentage of pores in soil. It is a key factor influencing soil permeability and surface runoff. The main steps of a porosity measurement experiment are as follows: ① the mass of soil sample at 120 mL is calculated using the soil density, and the mass of m_1 g water under this volume is calculated by using the moisture content of the sample; ② the TST-55 permeameter is used to get the m_2 g required water when the soil sample is saturated; and ③ since the density of water is 1 g/mL, the calculated porosity of the sample is $(m_1 + m_2)/120 \times 100\%$.

According to the above steps, the soil porosity was measured as shown in Figure 10:

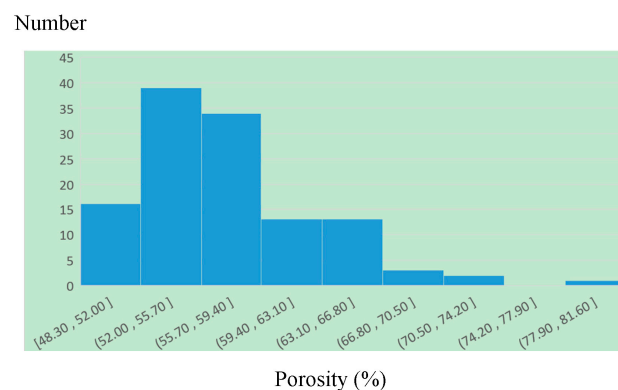


Figure 10. Histogram of fine sediment porosity.

It can be seen from the figure that the minimum porosity is 48.3% and the maximum is 81.6%, most of which is distributed between 52–59.4%.

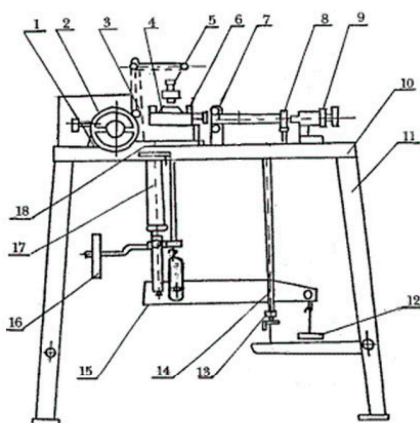
The results were exported into the database, and the correlation analysis of various parameters was carried out. As shown in Table 1, with a correlation coefficient of 0.70, the porosity was highly correlated with moisture in the study area. However, with a correlation coefficient of -0.51 , it was negatively correlated with the logarithm of the permeability coefficient.

(g) Shear strength measurement experiment

Soil shear strength refers to the ultimate strength of soil against shear stress, which mainly includes cohesion and internal friction angles.

Cohesion is the mutual attraction of adjacent objects within the same materials. The internal friction angle includes the surface friction of soil particles, the biting forces caused by the embedding and interlocking interactions between particles.

In this experiment, a ZJ strain-controlled direct shear instrument was used to measure cohesion and the internal friction angle, whose principle is shown in Figure 11.



1. Push seat; 2. Hand wheel A; 3. Bolt; 4. Shear box; 5. Pressure transmission screw
6. Screw bolt; 7. Force ring bearing; 8. Force ring; 9. Lock nut; 10. Baseboard;
11. Bracket; 12. Hanging tray; 13. Handwheel B; 14. Stud; 15. Lever;
16. Stationary hammer; 17. Extension bar; 18. Sliding frame

Figure 11. Principle of the ZJ strain-controlled direct shear instrument.

The steps are as follows: ① correct the lever to be horizontal; ② calculate the weight of the sample according to the volume of the ring knife of the direct shear instrument and the soil density, making a suitable sample for the shear instrument with its ring knife and then placing the shear box in the sliding frame, and pushing the soil sample into the shear box; ③ cover the cutting box, and press the screw on the cover; ④ tighten the force measuring ring and adjust the dial indicator to zero; ⑤ add weight loads or their combinations to the lever to obtain a series of shear normal stress of 50, 100, 200, and 300 kPa; ⑥ push the switch to the “cutting” to start cutting the sample; if the pointer no longer advances or begins to retreat, record the force ring readings immediately; ⑦ push the switch to the “back” direction and then take out the shear box and pour out the sheared soil sample, repeat steps ②–⑥ and do this four times on one sample upon which weight loads of 1.275 kg, 2.55 kg, 5.1 kg, and 7.65 kg are successively placed on the lever, and record the corresponding force ring readings (weight loads of 1.275 kg, 2.55 kg, 5.1 kg, and 7.65 kg represent shear-normal stresses of 50 kPa, 100 kPa, 200 kPa, and 300 kPa, respectively), and the shear strength can be converted by multiplying the force ring coefficient and its reading; and ⑧ display the measured four pairs of data in the coordinate system with σ as the horizontal axis and τ as the vertical axis to calculate its slope and intercept. The intercept of the straight line is cohesion C and the inclination angle of slope is the internal friction angle.

According to above steps, the histograms of cohesion and internal friction angle in the study area are shown in Figure 12.

It can be seen from the figure that the minimum cohesion is 13.95 kpa and the maximum is 39.55 kpa, most of which is between 20.35–26.75 kpa. The minimum internal friction angle is 16.16° and the maximum is 23.68°, most of which is between 18.98–21.8°. They both belong to the silt loams [34].

The results were exported into the database, and the correlation analysis of various parameters was carried out. As shown in Table 1, with correlation coefficients of -0.66 and -0.58 , the cohesion is negatively correlated with the internal friction angle and the logarithm of permeability coefficient, respectively. However, it is positively correlated with density with a correlation coefficient of 0.36.

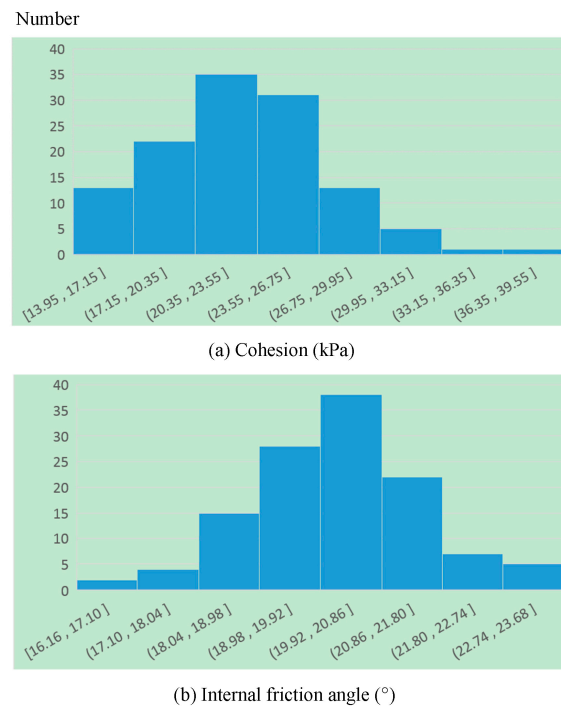


Figure 12. Histograms of fine sediment cohesion (a) and internal friction angle (b).

2.3.4. Data Standardization

Due to the different properties of each parameter, it usually has different dimensions and orders of magnitude. When the order of magnitude for each parameter varies greatly, the role of parameters with higher value in comprehensive analysis will be highlighted and that with a relatively lower value will be weakened. Therefore, it is necessary to standardize the original data using the following steps:

- (1) Calculate the average of each variable (mathematical expectation) \bar{x}_i and standard deviation s_i ;
- (2) Standardize data according to the following formula:

$$z_{ij} = (x - \bar{x}_i) / s_i$$

where z_{ij} is the standardized value, x_{ij} is the actual variable value, \bar{x}_i is the average, and s_i is the standard deviation.

2.4. Model

To establish the model between the permeability coefficient and its influencing factors, first the single factor analysis method was used to discover the most closely related factors. Then, the model between permeability coefficient and its influencing factors was established by the least-squares multivariate statistical analysis method.

(1) Selection of sensitive factors

To find the factors closely related to the permeability coefficient, we calculated the correlation coefficients between the permeability coefficient (p) and its influencing factors and sorted them from high to low. The results are shown in Table 2.

It can be seen from the table that cohesion, porosity, and density are most closely related to the permeability coefficient, with negative correlation coefficients.

Figure 13 shows the fitting relationships between the permeability coefficient and its influencing factors (cohesion, porosity, and density). The results show that the fitting effect between the logarithmic permeability coefficient and its influencing factors was better. Therefore, before multi-factor regression analysis, it is necessary to make a logarithmic transformation on the permeability coefficient to convert their nonlinear relationship into linear, and then carry out multiple linear regression analysis to improve the accuracy of the regression analysis.

Table 2. Table of correlation coefficients between permeability coefficient and its influencing factors.

No.	Influencing Factors	Permeability Coefficient (p, m/d)	ln(p) (m/d)
1	Cohesion (kPa)	−0.55681	−0.5834
2	Porosity (%)	−0.46196	−0.51413
3	Density (g/mL)	−0.45947	−0.51207
4	Moisture (%)	−0.42836	−0.4769
5	Internal friction angle (°)	0.323295	0.308409
6	K (%)	0.16128	0.195123
7	Fe (%)	0.113593	0.155239
8	Montmorillonite (%)	0.003181	−0.01579
9	Particle size (um)	0.002364	0.0011

(2) Multivariate regression analysis

The least-squares method is a mathematical optimization technology. It finds the best matching function of data by minimizing the sum of squared errors. The unknown data can be easily obtained by it, and the sum of squared errors between the obtained and the actual data can be minimized.

Its basic principles is:

$$f(x) = a_1\varphi_1(x) + a_2\varphi_2(x) + \dots + a_m\varphi_m(x)$$

where $\varphi_k(x)$ is a set of linearly independent functions, a_k is the undetermined coefficient ($k = 1, 2 \dots, m$), and the fitting criterion is to minimize the sum of the square distance between the measured value y_i and the predicted value $f(x_i)$, which is also named as the least-square criterion.

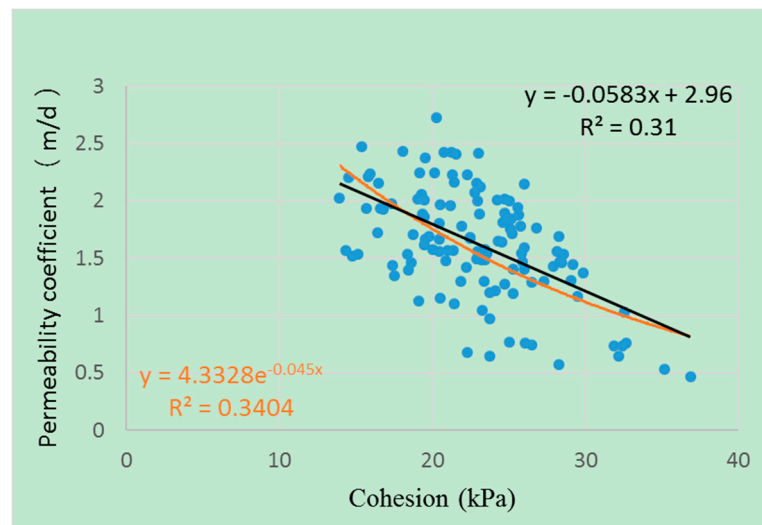
Let (x, y) be a pair of observations, and $x = [x_1, x_2 \dots, x_n]^T \in \mathbb{R}^n$, $y \in \mathbb{R}$, which satisfies the following functions:

$$y = f(x, w)$$

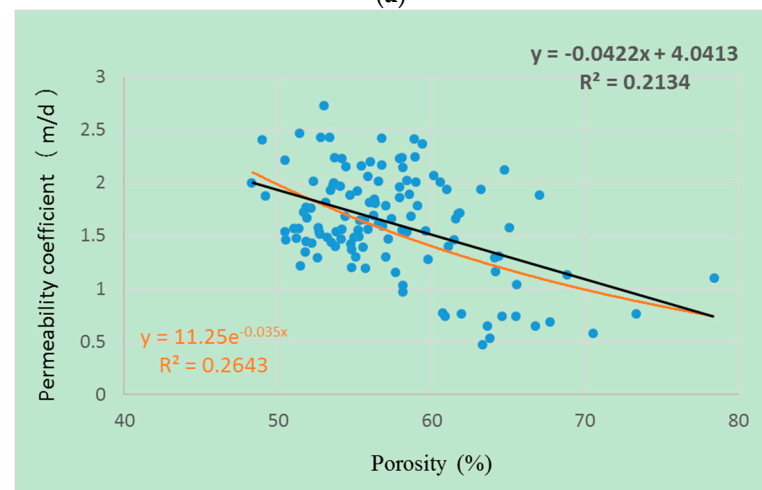
where $w = [w_1, w_2 \dots, w_n]^T$ is an unknown parameter. To find the optimal estimate of the parameter w for a serials of given datasets (x_i, y_i) , the objective function can be solved as:

$$L(y, f(x, w)) = \sum_{i=1}^n |y_i - f(x_i, w_i)|^2 \quad (2)$$

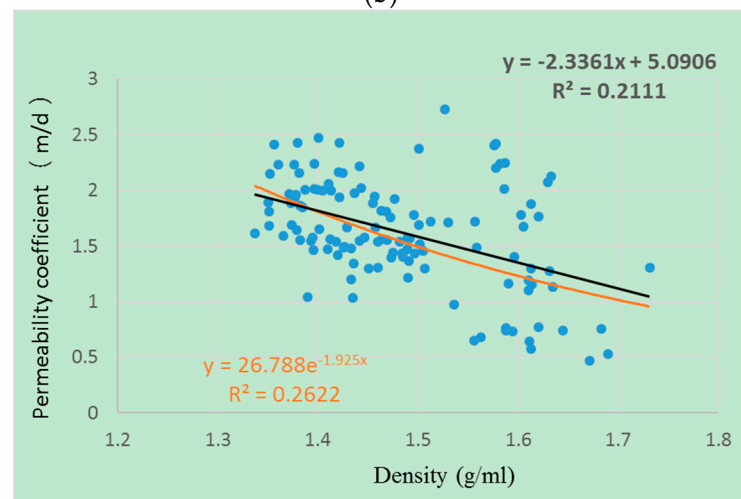
Parameters w_i ($i = 1, 2 \dots, n$) can be determined when minimizing the value of objective function.



(a)



(b)



(c)

Figure 13. Fitting relationships between the permeability coefficient and cohesion (a), porosity (b), and density (c) in which the black lines and equations are of linear relationships, while brown lines and equations are of exponential relationships.

3. Results

According to the above analysis, the formula between the logarithm of the permeability coefficient and three standardized influencing factors, namely cohesion, porosity, and density, is established by the least-squares method as follows:

$$\ln(p) = 0.1875 - 0.0387x_1 - 0.0455x_2 - 0.0619x_3 \quad (3)$$

where p is the permeability coefficient, x_1 is the standardized density, x_2 is the standardized porosity, and x_3 is the standardized cohesion.

The fitting relationship between the measured and the predicted values is shown in Figure 14.

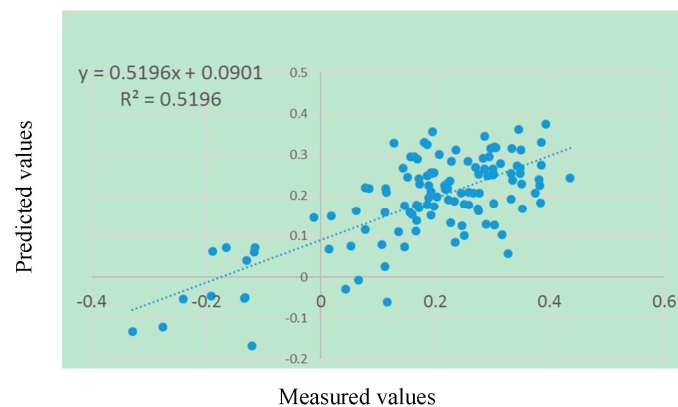


Figure 14. The fitting relationship between the measured and the predicted values of $\ln p$ (p : permeability coefficient) using the model. Spatial distribution and the determination coefficient (R^2) show a good data-fitting effect.

As can be seen from Figure 14, the determination coefficient (R^2) of the model is 0.5196. The t-test for each regression coefficient is shown in Table 3, with p values of each regression coefficient less than 0.01, indicating that the influencing factors (cohesion, porosity, and density) have extremely significant correlation with the permeability coefficient in the probability of 99.99%, and the model has a good prediction ability.

Table 3. T-test table for regression coefficients.

	Coefficient	p Value	Lower Limit 95%	Upper Limit 95%
Intercept	0.1875	6.53×10^{-38}	0.16814	0.20687
Density	-0.0387	0.00063	-0.0605	-0.01688
Porosity	-0.0455	4.77×10^{-5}	-0.06679	-0.02415
Cohesion	-0.0619	5.44×10^{-8}	-0.08295	-0.04079

4. Discussion

From the model, we can see that cohesion is the closest factor to the permeability coefficient, followed by porosity and density, which are negatively related. The reasons are as follows:

(1) With an exponentially negative correlation, the relationship between cohesion and the permeability coefficient is very close.

Cohesion is the mutual attraction between adjacent objects within the same material. It mainly includes electrostatic attraction, van der Waals forces, cementation chemical bonds between particles, valence bonds of indirect contact of particles, apparent cohesion, etc. Physically, it represents the shear strength of the failure surface without any normal stress. The greater the cohesion is, the stronger the attraction between the particles becomes and the greater the resistance when water flows through the soil, which leads to the small permeability coefficient.

(2) With an exponentially negative correlation, the relationship between porosity and the permeability coefficient is close.

Soil is a kind of geotechnical material with porous media, and its micro pore structure determines its macro permeability [35]. The main clay mineral in the study area is montmorillonite, which is characterized by strong water absorption. In the case of a fixed volume, the larger the porosity is, the easier it is to adsorb water. When most of the pores between clay particles are occupied by bound water, soil moisture increases, while the large to medium sized pores decrease, thus leading to the permeability coefficient reducing [33].

(3) With an exponentially negative correlation, the relationship between density and the permeability coefficient is close.

When the total sediments mass is fixed, the greater the density is and the smaller the volume becomes, indicating that the soil compactness is higher, which compresses the gap between the soil particle skeleton and reduces the infiltration speed of water and thus leads to a smaller permeability coefficient [36–39].

(4) The relationship between particle size and permeability coefficient is not significant in the study area.

Previous research showed that there was an exponentially negative correlation between the particle size of silt sediments and the permeability coefficient, while there was an exponentially positive correlation between the particle size of sand sediments and the permeability coefficient [40]. This phenomenon shows that the relationship between the permeability coefficient and particle size cannot show a simple function, but is affected by many factors. As in the study area, coarse particles only play the role of skeleton, while fine particles have significant impact on the permeability coefficient: the increase of fine particles will not only reduce the skeleton effect of coarse particles, but also increase their van der Waals forces, thus enhancing the electrostatic water attractions. Furthermore, it weakens the ability of water molecules to engage in free movement, which increases the water molecules adsorbed on the soil particles surface. The increase of fine particles will increase the blocking probability of the seepage channel and affect the permeability coefficient [41]. Because fine sediments in the study area are mainly silt loams, their permeability is not only influenced by particle size, but also by silt content, clay content, etc. As a result, the relationship between the permeability coefficient and particle size is complex and does not show a significant correlation in the study area.

5. Summary and Conclusions

To summarize the permeability characteristics of fine sediments in debris-flow gullies of Laobeichuan County and analyze the influencing factors to establish the quantitative model between them, we carried out soil measurement experiments. The measured parameters mainly included the permeability coefficient and its influencing factors, such as density, moisture, minerals, elements, particle size, porosity, and shear strength. Based on the above data, the main influencing factors controlling the permeability coefficient were discovered, and the model between them was established. The main conclusions are as follows:

(1) The characteristics of fine sediments in debris-flow gullies of Laobeichuan County are summarized.

The fine sediments of debris-flow gullies in Laobeichuan County are mainly silt loams, and their permeability coefficients are concentrated in 1.15–2.17 m/d, belonging to the category of medium permeability. They are stable under the conditions of non-heavy rain. The particle size is mainly in the range of 10–20 μm , which has no significant relationship with the permeability coefficient. The density is mainly in the range of 1.34–1.54 g/mL, which is significantly related to the permeability coefficient. The moisture is mainly in the range of 4.01–12.02%, which is closely related to density, porosity, montmorillonite, and the permeability coefficient. The porosity is mainly in the range of 52–59.4%, which is closely related to moisture and the permeability coefficient. The cohesion is mainly in the range

of 20.35–26.75 kPa, and the internal friction angle is in the range of 18.98–21.8°, which are closely related to the permeability coefficient and density.

(2) The influencing factors of the fine sediment permeability coefficient were discovered in the study area.

Results show that the cohesion was the closest parameter to the permeability coefficient in Laobeichuan County, followed by porosity and density. This is mainly because ① the greater the cohesion is, the bigger the mutual attraction between soil particles becomes, and the greater the resistance to be overcome when water passes through soil, thus resulting in the reduction of permeability coefficient; ② a soil pore is a place of water movement and storage; it is the key factor affecting soil permeability and determining surface runoff time and there was a positive correlation between soil porosity and moisture (with a correlation coefficient of 0.70) and a negative correlation with the logarithm of permeability coefficient (with a correlation coefficient of -0.51), mainly because the main clay mineral in the study area is montmorillonite and, as we know, montmorillonite has the characteristics of strong water absorption and easy expansion after water absorption. In the case of a fixed volume, the greater the porosity becomes, the easier it is to adsorb water, which results in the higher moisture. Because the combined water occupies a large number of pores, the effective channel of seepage greatly reduces, which results in the deterioration of the permeability coefficient [36]; in addition, the pore size between clays is very small and a large number of capillaries are formed. The siphon effect of capillaries will increase the resistance to the decline of water flow and thus reduce the permeability coefficient. ③ The soil density has a positive correlation with moisture (with a correlation coefficient of 0.80) and a negative correlation with the logarithm of the permeability coefficient (with a correlation coefficient of -0.51). This is mainly because, in the case of a fixed volume, the higher the moisture is, the heavier the weight of the sample becomes, which results in a greater soil density. When the total porosity is fixed, the higher the moisture is, the smaller the residual soil porosity becomes, which results in a low soil permeability coefficient.

(3) A model between the permeability coefficient and its influencing factors of fine sediments was established in the study area.

A model between the permeability coefficient and its influencing factors (cohesion, porosity and density) of debris-flow gullies in Laobeichuan County was established by the least-squares multivariate statistical analysis method. The results show that cohesion is the closest parameter to the permeability coefficient, followed by porosity and density, which are exponentially negatively correlated. The results show that the determination coefficient of the model is 0.5196, which indicates that the corresponding correlation coefficient is 0.72. Each influencing factor passed the t-test and was significantly correlated with the permeability coefficient with a probability of 99.99%. Therefore, the model has a good prediction ability. It not only provides a theoretical basis for analyzing the stability of the fine sediments of debris-flow gullies in Laobeichuan County, but also points out the direction for detecting the stability of fine sediments in debris-flow gullies.

Author Contributions: Conceptualization, Q.W. and J.X.; methodology, Q.W., J.X., J.Y. and P.L.; validation, Q.W., J.X. and P.L.; formal analysis, Q.W. and J.X.; investigation, Q.W., J.X., P.L., D.C. and W.X.; data curation, J.X., J.Y. and P.L.; writing—original draft preparation, Q.W., J.X. and J.Y.; writing—review and editing, Q.W.; visualization, D.C.; supervision, W.X.; project administration, Q.W.; funding acquisition, Q.W. All authors have read and agreed to the published version of the manuscript.

Funding: This research was funded in part by the National Natural Science Foundation of China, grant number 42071312, in part by the Hainan Hundred Special Project, grant number 31, JTT [2018], in part by the National Key R&D Program, grant number 2021YFB3900503, and in part by “the Special Project of Strategic Leading Science and Technology of the Chinese Academy of Sciences, grant number XDA19070202”.

Institutional Review Board Statement: Not available.

Informed Consent Statement: Not available.

Data Availability Statement: Not available.

Conflicts of Interest: The authors declare no conflict of interest.

References

1. Liu, P.; Wei, Y.M.; Wang, Q.J.; Xie, J.J.; Chen, Y.; Li, Z.C.; Zhou, H.Y. A research on landslides automatic extraction model based on the improved mask R-CNN. *ISPRS Int. J. Geo-Inf.* **2021**, *10*, 168. [[CrossRef](#)]
2. Xiao, J.B. The Emergency Management Department of China Announced the National Top Ten Disasters in 2019. Available online: <http://society.people.com.cn/n1/2020/0112/c1008-31544517.html,2020> (accessed on 2 January 2022).
3. Liu, D.Y.; Yu, K. Zhouqu: Why did “Longshang Jiangnan” become a muddy city. *Land Resour. Guide* **2010**, *9*, 20–21.
4. Tang, C.; Liang, J.T. Study on characteristics of 9.24 rainstorm and debris flow in Beichuan, Wenchuan earthquake area. *J. Eng. Geol.* **2008**, *16*, 751–758.
5. Wu, Q.; Xu, L.R.; Zhou, K.; Liu, Z.Q. Starting analysis of loose deposits of gully debris flow. *J. Nat. Disasters* **2015**, *24*, 89–97.
6. Xu, X.C.; Chen, J.P.; Shan, B. Study of grain distribution characteristics of solid accumulation in debris flow. *Yangtze River* **2015**, *46*, 51–54.
7. Ma, M. Stability analysis of high slope of accumulation at the outlet of pressure flood discharge and sediment discharge tunnel of Jiudianxia Water Control Project. *Water Conserv. Plan. Des.* **2019**, *4*, 64–67.
8. Tang, M.G.; Xu, Q.; Li, J.Q.; Luo, J.; Kuang, Y. An experimental study of the failure mechanism of shallow landslides after earthquake triggered by rainfall. *Hydrogeol. Eng. Geol.* **2016**, *43*, 128–135.
9. Jonathan, W.F.R.; Reuben, A.H.; Brian, S.I. Particle size distribution of main-channel-bed sediments along the upper Mississippi River, USA. *Geomorphology* **2016**, *264*, 118–131.
10. Xie, J.; Wang, M.; Liu, K.; Coulthard, T.J. Modeling sediment movement and channel response to rainfall variability after a major earthquake. *Geomorphology* **2018**, *320*, 18–32. [[CrossRef](#)]
11. Marcel, H.; Velio, C.; Coraline, B.; Guo, X.; Berti, M.; Graf, C.; Hübl, J.; Miyata, S.; Smith, J.B.; Yin, H.-Y. Debris-flow monitoring and warning: Review and examples. *Earth-Sci. Rev.* **2019**, *199*, 102981. [[CrossRef](#)]
12. Dobrokhotov, V.; Oakes, L.; Sowell, D.; Larin, A.; Hall, J.; Kengne, A.; Bakharev, P.; Corti, G.; Cantrell, T.; Prakash, T.; et al. Toward the nanospring-based artificial olfactory system for trace-detection of flammable and explosive vapors. *Sens. Actuators B Chem.* **2012**, *168*, 138–148. [[CrossRef](#)]
13. Philip, K.L.; Lalit, K.; Richard, K. Monitoring river channel dynamics using remote sensing and GIS techniques. *Geomorphology* **2019**, *325*, 92–102.
14. Miao, Q.H.; Yang, D.W.; Yang, H.B.; Li, Z. Establishing a rainfall threshold for flash flood warnings in China’s mountainous areas based on a distributed hydrological model. *J. Hydrol.* **2016**, *541*, 371–386. [[CrossRef](#)]
15. Wang, Q.J.; Wei, Y.M.; Chen, Y.; Lin, Q.Z. Hyperspectral Soil Dispersion Model for the Source Region of the Zhouqu Debris Flow, Gansu, China. *IEEE J. Sel. Top. Appl. Earth Obs. Remote Sens.* **2016**, *9*, 876–883. [[CrossRef](#)]
16. Fan, R.L.; Zhang, L.M.; Wang, H.J.; Fan, X.M. Evolution of debris flow activities in Gaojiagou Ravine during 2008–2016 after the Wenchuan earthquake. *Eng. Geol.* **2018**, *235*, 1–10. [[CrossRef](#)]
17. Hu, W.; Scaringi, G.; Xu, Q.; Pei, Z.; Van Asch, T.W.; Hicher, P.-Y. Sensitivity of the initiation and runout of flowslides in loose granular deposits to the content of small particles: An insight from flume tests. *Eng. Geol.* **2017**, *231*, 34–44. [[CrossRef](#)]
18. Liu, Y. Study on test method of permeability coefficient of cohesionless coarse-grained soil in hydraulic engineering. *Shanxi Water Conserv.* **2020**, *12*, 211–213.
19. Bayat, B.; Van, D.T.C.; Yang, P.Q.; Verhoef, W. Extending the SCOPE model to combine optical reflectance and soil moisture observations for remote sensing of ecosystem functioning under water stress conditions. *Remote Sens. Environ.* **2019**, *221*, 286–301. [[CrossRef](#)]
20. Elzbieta, R.; Maciej, D.; Kazimierz, K. Sediment budget of high mountain stream channels in an arid zone (High Atlas mountains, Morocco). *Catena* **2020**, *190*, 104530. [[CrossRef](#)]
21. Jiang, F.; Zhan, Z.; Chen, J.; Lin, J.; Wang, M.K.; Ge, H.; Huang, Y. Rill erosion processes on a steep colluvial deposit slope under heavy rainfall in flume experiments with artificial rain. *Catena* **2018**, *169*, 46–58. [[CrossRef](#)]
22. Friedl, F.; Weitbrecht, V.; Robert, M.B. Erosion pattern of artificial gravel deposits. *Int. J. Sediment Res.* **2018**, *33*, 57–67. [[CrossRef](#)]
23. Wei, J.; Shi, B.L.; Li, J.L.; Li, S.S.; He, X.B. Shear strength of purple soil bunds under different soil water contents and dry densities: A case study in the Three Gorges Reservoir Area, China. *Catena* **2018**, *166*, 124–133. [[CrossRef](#)]
24. Lin, J.; Huang, Y.; Zhao, G.; Jiang, F.; Wang, M.-K.; Ge, H. Flow-driven soil erosion processes and the size selectivity of eroded sediment on steep slopes using colluvial deposits in a permanent gully. *Catena* **2017**, *157*, 47–57. [[CrossRef](#)]
25. Li, M.W.; Tang, C.; Chen, M. Spatio-temporal evolution characteristics of landslides in debris flow catchment in Beichuan County in the Wenchuan earthquake zone. *Hydrogeol. Eng. Geol.* **2020**, *47*, 182–190.
26. Li, C.X.; Ma, Y.; He, Y.X. Sensitivity analysis of debris flow to environmental factors: A case of Longxi River basin in Duijiangyan, Sichuan Province. *Chin. J. Geol. Hazard Control* **2020**, *31*, 32–39.
27. Ye, L. The Relationship between the Distribution of Debris Flow and Environmental factors—A Case Study of Counties in Northern Mianyang City. *J. Baoshan Univ.* **2021**, *40*, 64–70.

28. Yang, B.X.; Cao, D.J. The technology innovation and inspiration of “GF-2” satellite high-resolution camera. *Spacecr. Recovery Remote Sens.* **2015**, *36*, 10–15.
29. Yin, Y.P.; Zhang, Z.C.; Zhang, M.S.; Zheng, W.M.; Wei, L.W.; Wu, S.R.; Zhang, R.S.; Yao, X.; Zhang, K.J.; Li, X.C.; et al. *Geological and Mineral Industry Standard of the People’s Republic of China: Code for Investigation of Landslide, Collapse and Debris Flow Disasters 1:50,000 (DZ/T 02161-2014)*; China Standards Press: Beijing, China, 2015.
30. Xu, M.; Yang, L.Z.; Wang, D.H.; Chen, M.J.; Chu, W.Y. *National Standard of the People’s Republic of China: Technical Guide for Soil Sampling of Soil Quality (GB/T 36197-2018)*; China National Standardization Administration Committee: Beijing, China, 2018.
31. Sheng, S.X.; Dou, Y.; Tao, X.Z.; Zhu, S.Z.; Xu, B.M.; Li, Q.Y.; Guo, X.L.; He, X.M. *National Standard of the People’s Republic of China: Geotechnical Test Code (SL237-1999)*; China Water Resources and Hydropower Press: Beijing, China, 1999.
32. Li, C.M.; Wang, D.; Liu, X.L.; Tan, M.J.; Liu, Y.; Jin, Z.G.; Yin, Y.; Wu, Y.J.; Qiu, R.Q.; Sun, W.; et al. *National Standard of the People’s Republic of China: Basic Provisions for Basic Geographic Information Database (GB/T 30319-2013)*; China National Standardization Administration Committee: Beijing, China, 2013.
33. Fan, M.Q.; Teng, Y.J.; Wu, W.; Liu, Y.H.; Luo, M.Y.; Wang, Y.; Xin, H.B.; Zhang, W.; Wen, Y.F.; Gong, B.W.; et al. *Engineering Classification Standard for Soil (GB/T 50145-2007)*; China Planning Press: Beijing, China, 2008.
34. Sun, X.D.; Wang, D. Analysis of cohesion value of soil. *Liaon. Build. Mater.* **2010**, *3*, 39–42.
35. Zhang, X.J.; Liu, P.; Yang, X.Q.; Wang, Y. A Study of the Relationship between Permeability and Pore Structure of Lime-treated Loess. *J. Guangdong Univ. Technol.* **2021**, *38*, 97–105.
36. Liu, H.W.; Dang, F.N.; Tian, W.; Mao, L.M. Prediction of permeability of clay by modified Kozeny—Carman equation. *Chin. J. Geotech. Eng.* **2021**, *43* (Suppl. S1), 186–191.
37. Fan, G.Y.; Zhang, J.M.; Shen, J.B. Laboratory study on penetration resistance of sandy soil modified in high sandy soil area. *Shanxi Archit.* **2021**, *47*, 68–70.
38. Hou, Y.B.; Qiao, D.X. Influence of Compaction on Strength and Permeability of Total Tailings Consolidation Body. *Met. Mine* **2021**, *10*, 67–74.
39. Charlotte, J.W.V.V.; Julia, G. Effect of compaction and soil moisture on the effective permeability of sands for use in methane oxidation systems. *Waste Manag.* **2020**, *107*, 44–53.
40. Wang, S. Study on Seepage Law of Riverbed in Desert Section of Hotan River. Master’s Thesis, Tarim University, Xinjiang, China, 2021.
41. Yu, J. Study on Permeability Characteristics and Fine Particle Migration Law of Deposited Soil in Debris Flow Channel. Master’s Thesis, Sichuan Normal University, Chengdu, China, 2020.